

Measurement of Higgs production in association with high p_T jets with the ATLAS detector

Bruce Mellado¹

University of the Witwatersrand, 1 Jan Smuts Avenue, Johannesburg 2000, South Africa

Abstract. The first measurement of the differential cross section of the Higgs boson, performed in the diphoton decay channel, is presented. The dataset used corresponds to 20.3 fb^{-1} of proton-proton collisions at the center of mass of 8 TeV, produced by the LHC and collected by the ATLAS detector in 2012. With its high signal selection efficiency the diphoton decay channel is well suited to probe the underlying kinematic properties of the signal production and decay. Measurements for several diphoton and jet distributions are made for isolated photons within the geometric acceptance of the detector and they are corrected for experimental acceptance and resolution. Results are compared to theoretical predictions at the particle level. Prospects for Run 2 are discussed.

1. Introduction

In the Standard Model, SM, of electro-weak, EW, and strong interactions, there are four types of gauge vector bosons (gluon, photon, W and Z) and twelve types of fermions (six quarks and six leptons) [1, 2, 3, 4]. These particles have been observed experimentally. At present, all the data obtained from the many experiments in particle physics are in agreement with the Standard Model. In the Standard Model, there is one particle, the Higgs boson field, that is responsible for giving masses to all the elementary particles [5, 6, 7, 8]. In this sense, the Higgs particle occupies a unique position.

In July 2012 the ATLAS and CMS experiments reported the discovery of a boson, a Higgs-like particle with a mass $m_H \approx 125 \text{ GeV}$ based on the data accumulated during 2011 and part of 2012 periods [9, 10]. It is also relevant to note that no additional Higgs bosons with couplings as in the Standard Model have been observed in the range of $m_H < 600 \text{ GeV}$.

The interest of the community has now shifted towards understanding the properties of the newly discovered boson. One of the relevant aspects is the production of the Higgs boson in association with high transverse momentum, p_T , hadronic jets. Together with the exploration of inclusive kinematics these measurements are a test of the SM. Some of these observables are sensitive to physics beyond the SM. Ultimately, the detailed measurement of the Higgs boson in association with jets will help improve the uncertainty of this important background to the extraction of the Vector Boson Fusion (VBF) mechanism. This production mechanism entails the scattering of two energetic quarks that exchange a weak boson. This weak boson radiates a Higgs boson. This production mechanism displays two high p_T jets at leading order and with a very particular topological configuration. Presence of admixtures of nonanomalous couplings in the

¹ E-mail: Bruce.Mellado@wits.ac.za

$HVV, V = Z, W$ vertex would lead to the distortion of the kinematic pattern, opening a window of opportunity to potentially observe physics beyond the SM [11, 12].

The results shown here are the first of their kind and were reported by the ATLAS collaboration in Ref. [13]. In section 2 the event selection, definition of fiducial cuts and a summary of the systematic errors are described. In section 3 the unfolding procedure is briefly outlined. Section 4 shows differential cross-section distributions for relevant observables. The note is concluded with a brief summary and conclusions in section 5.

2. Event Selection and Systematic Errors

The event and object selection used in this analysis follow closely the approach of earlier ATLAS analyses. This includes the generation of Monte Carlo (MC) events. Events are recorded using a diphoton trigger with an efficiency above 99% with respect to the offline selection, requiring two energetic clusters that match criteria according to expectations for photon-induced electromagnetic showers. One of the clusters must have transverse energy, E_T , greater than 35 GeV, and the other one must be greater than 25 GeV. They must lie within the fiducial acceptance of $|\eta| < 2.37$, where η is the pseudorapidity, excluding the transition region between the barrel and endcap calorimeters, $1.37 < |\eta| < 1.56$. Basic data quality requirements ensure that all necessary components of the detector are operational. Each photon of the pair must further satisfy isolation requirements for the inner detector and calorimeter. The total energy in a cone around the photon of $\Delta R < 0.4$ must be less than 6 GeV.

MC generation is an important element to the analysis. Particle level description of the final state is defined after the process of hadronization in the MC. The particle level fiducial definition is chosen to mirror the event selection in data. This minimizes the extrapolation from detector level to particle level quantities. The selection criteria are as follows: the two highest- E_T , isolated final state photons, within $|\eta| < 2.37$ and with $105 \text{ GeV} < m_{\gamma\gamma} < 160 \text{ GeV}$ are selected. Note that the transition region between the barrel and endcap calorimeters is not removed in this definition. After the pair is selected, the same cut on $E_T/m_{\gamma\gamma}$ is applied as in the event selection in data: $E_T/m_{\gamma\gamma} > 0.35(0.25)$ for the higher- E_T (lower- E_T) photon. The isolation criterion is defined as follows: the sum of the p_T of all stable particles excluding muons and neutrinos is required to be less than 14 GeV within $\Delta R < 0.4$ of the photon. This requirement was found to correspond approximately to the calorimetric isolation cut of 6 GeV at reconstruction level.

Jets are selected both at particle and reconstruction level, using the anti-kt algorithm with a distance parameter of $R = 0.4$. At reconstruction level, the inputs are clusters of energy in the electromagnetic and hadronic calorimeters. At particle level all stable particles excluding muons and neutrinos serve as input. The jet must have transverse momentum exceeding 30 GeV, and rapidity $|y| < 4.4$.

A comprehensive set of systematic uncertainties are considered. This is comprised of three groups:

- Uncertainties on the signal yield. These include systematics on the luminosity, trigger and isolation efficiencies.
- Uncertainties on photon energy resolution.
- Migration uncertainties. These include the jet energy resolution, jet energy scale, the jet vertex fraction ² and jets from pileup

A summary of the size of all uncertainties considered and those that are neglected can be found in Ref. [13].

² The jet vertex fraction is introduced as a measure to quantify the probability that a jet originates from the primary vertex and not from other collisions in the event.

3. Unfolding Procedure

The data yields extracted are corrected for detector effects using bin-by-bin factors. These are derived as the ratio of the yields from particle level to reconstruction level from simulated Higgs boson events, according to the SM expectation. In each bin,

$$c_i = n_i^{Particle\ level} / n_i^{Reconstructed} \quad (1)$$

is used to correct the extracted signal yield obtained in the data. This unfolding procedure corrects for all efficiencies, acceptances, and resolution effects. The correction factors range from 1.2 to 1.8, and include the extrapolation (about 20%, across all bins and observables) over the small region in rapidity (see section 2) excluded from reconstructed photon candidates. The method is formally unbiased provided that $c^{MC} = c^{Data}$. In practice, the requirement to use this method is that the purity of events reconstructed into the same bin in which they were generated should not be significantly below 50%.

The application of the unfolding coefficients defined in expression 1 assumes that the Higgs is produced as predicted by the SM. This feature of the measurement unavoidably results in the generation of certain biases. These biases need to be quantified and can be classified into sample composition and shape. Four groups of variations that are orthogonal to each other, are considered:

- Apply scale factors to the various production mechanisms according to measurements of their signal strengths at ATLAS. This check ensures that assuming the SM with regards to the relative rate of various production mechanisms does not generate significant biases.
- Impact of missing higher order perturbative corrections in gluon-gluon fusion production.
- Disable multi-parton interactions to test the impact of the modelling of the underlying event.
- Reweight the combined SM prediction in $p_T^{\gamma\gamma}$ and $|y^{\gamma\gamma}|$ or $p_T^{j_1}$ spectra (see section 4) to match the unfolded results in these variables. This check ensures that the shape of the differential distribution predicted by the SM does not bias the measurement.

A complete study of these biases is reported in Ref. [13]. Overall, the measurement is dominated by statistical uncertainties. At this point in time model dependencies do not play a critical role.

4. Results

Figure 1 displays the measured differential cross-sections for inclusive observables: the Higgs boson candidate transverse momentum, $p_T^{\gamma\gamma}$, its rapidity $|y^{\gamma\gamma}|$ and the helicity angle $|\cos(\theta^*)|$. The lower right plot displays the transverse momentum of the leading jet in the event, $p_T^{j_1}$. Figure 2 shows the results of jet-related quantities: the exclusive rate of jets for events with up to three jets, the ratio of the exclusive rate to the inclusive rate, $\sigma_i/\sigma_{\geq i}$, the azimuthal angle difference between the two leading jets in the event, $\Delta\phi_{jj}$, and the transverse momentum of the di-photon and di-jet system in events with at least two jets, $p_T^{\gamma\gamma jj}$.

Results are reported for the region of the phase-space described in section 2. The results are compared to MC predictions with the SM expectation. All predictions were generated at $m_H = 126.8$ GeV, the central value of the measured Higgs boson mass in the diphoton channel by ATLAS. For the gluon-gluon fusion mechanism three different predictions are considered: Higgs boson production at NLO POWHEG [14], Higgs boson + 1 jet from MINLO [15] at NLO, and HRes at NNLO+NNLL [16]. The POWHEG prediction is shown for all 8 observables. HRes is presented for $p_T^{\gamma\gamma}$ and $|y^{\gamma\gamma}|$, and MINLO is used for the remaining 6 observables.

The measurements reported here are limited by statistical uncertainties. A statistical analysis to quantify the compatibility of the data with the SM prediction, including the Higgs boson p_T

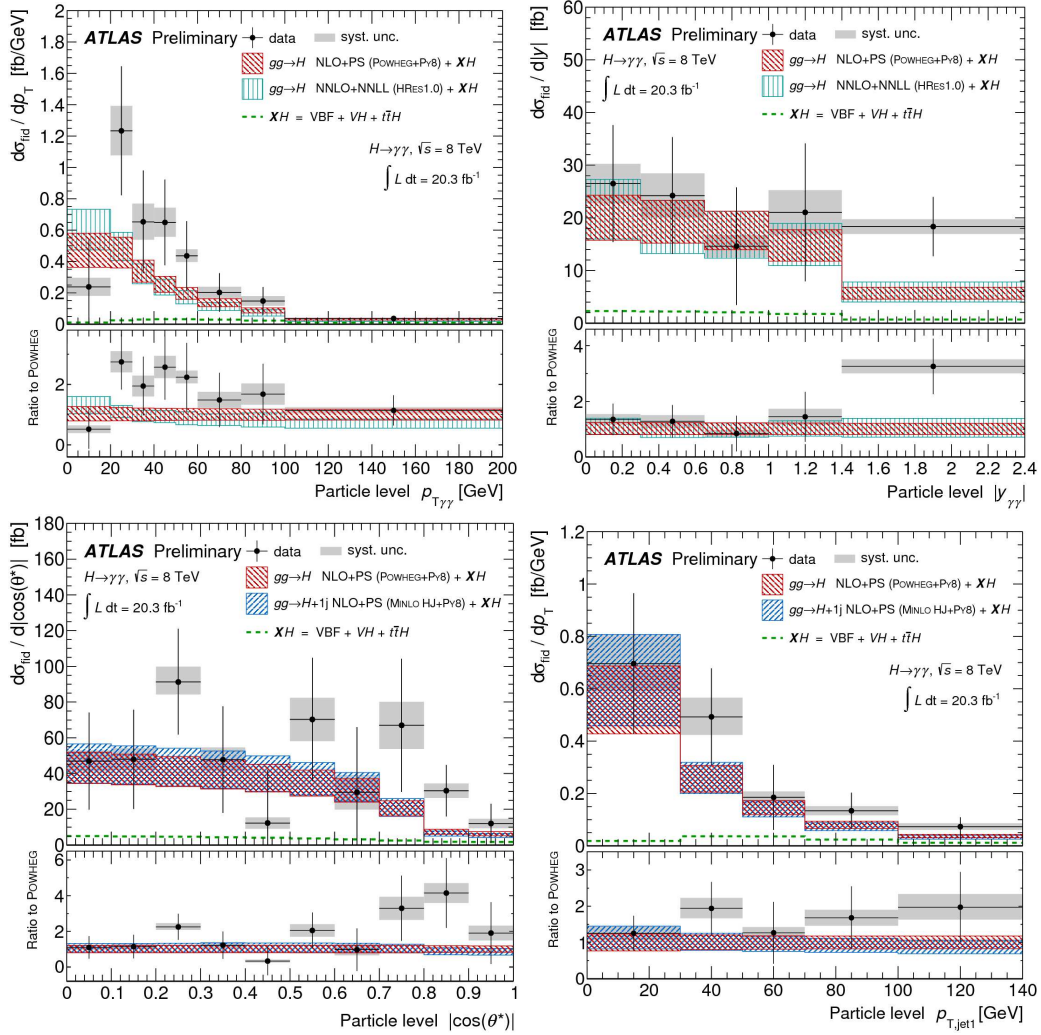


Figure 1. Observed differential cross sections of the Higgs bosons decaying into two isolated photons. Systematic uncertainties are presented in grey, and the black bars represent the quadratic sum of statistical and systematic errors. The hatched histograms present theoretical predictions for the Standard Model at $\sqrt{s} = 8$ TeV and $m_H = 126.8$ GeV. Their width represents the theory uncertainties from missing higher order corrections, the PDF set used, the simulation of the underlying event, and the branching fraction. The sum of VBF with WH , ZH , and ttH is denoted XH . These are added to the simulated ggH predictions from POWHEG, MINLO, and HRes (see text).

distribution. The compatibility of the data and MC is better than 10%. One can conclude that the reported measurements are consistent with the predictions by the SM within uncertainties.

5. Summary and Conclusions

Following the discovery of a new scalar boson, the measurement of properties becomes a focus of investigation by the experimentalists. The measurement of differential cross-sections of inclusive observables and the production in association with hadronic jets represents a test of the SM and a window of opportunity for searches of physics beyond.

The measurements reported here are the first of its kind. The comparison of these

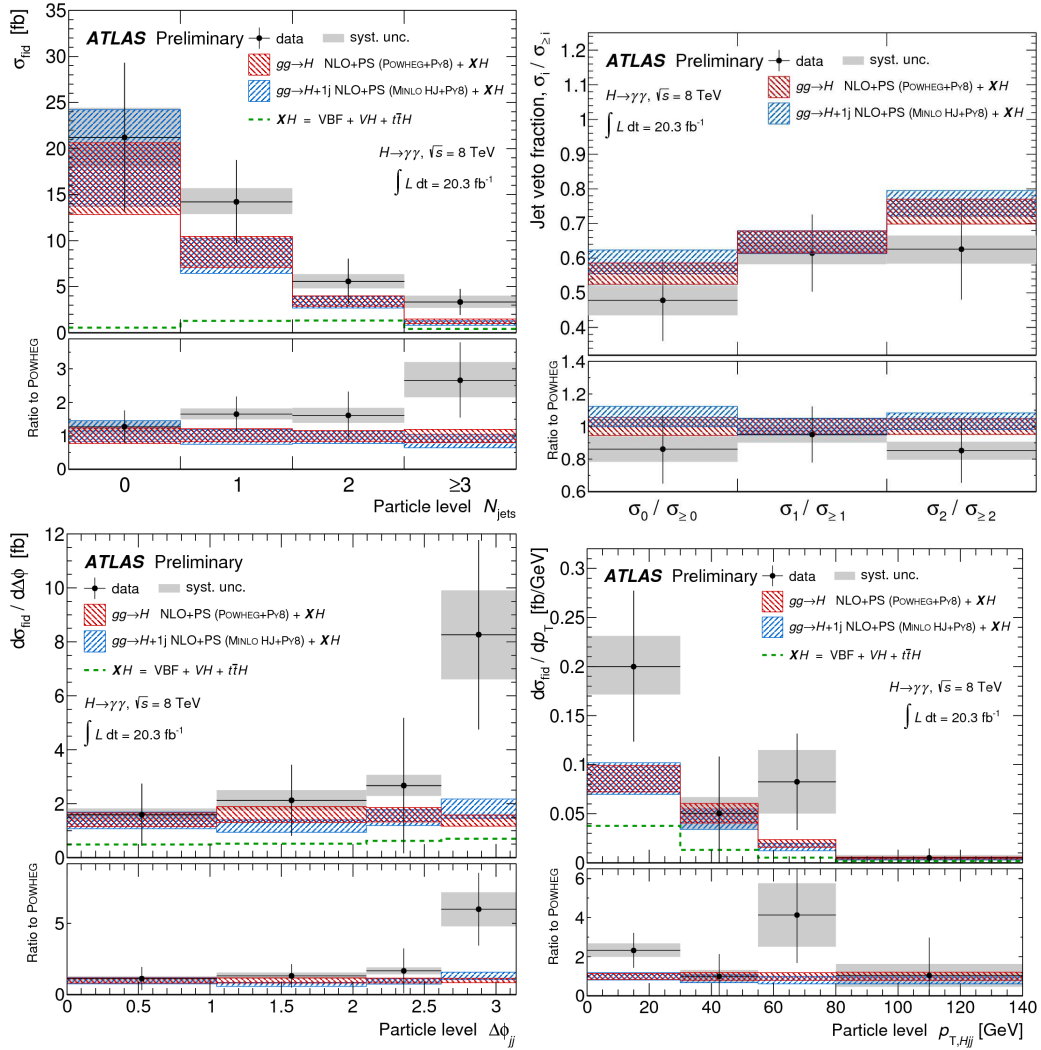


Figure 2. Same as Fig. 1 for multi-jet related variables (see text).

measurement with state-of-the-art MC tools and calculations indicate that Higgs kinematics and that of the associated jets are consistent with the SM within the errors quoted. This measurement needs to be taken as a first step towards the establishment of precision measurements that will lead to the reduction of the uncertainties in the understanding of the Higgs production via gluon-gluon fusion in association with jets. This will be essential in furthering the accuracy of the measurements of the Higgs production in VBF.

The measurements presented here are limited by the statistical uncertainty. The prospects of re-doing these measurements with Run 2 data are very exciting. With the increased proton-proton center of mass energy the Higgs production cross-section in certain corners of the phase-space will increase considerably. These effects, in addition to the collection of about 4-5 times the integrated luminosity, render Run 2 a very exciting period for the exploration of Higgs boson physics at the LHC.

References

- [1] Glashow S 1961 *Nucl.Phys.* **22** 579

- [2] Weinberg S 1967 *Phys.Rev.Lett.* **19** 1264
- [3] Salam A 1968 Proceedings to the eighth nobel symposium, may 1968, ed: N. svartholm 357
- [4] Glashow S , Iliopoulos J and Maiani L 1970 *Phys.Rev.* **D2**, 1285
- [5] Englert F and Brout R 1964 *Phys.Rev.Lett.* **13** 321
- [6] Higgs P 1964 *Phys.Lett.* **12** 132
- [7] Higgs P 1964 *Phys.Rev.Lett.* **13** 508
- [8] Guralnik G, Hagen C and Kibble T 1964 *Phys.Rev.Lett.* **13** 585
- [9] ATLAS Collaboration (G. Aad *et al.*) 2012 *Phys.Lett.* **B716** 1
- [10] CMS Collaboration (S. Chatrchyan *et al.*) 2012 *Phys.Lett.* **B716** 30
- [11] Englert C, Goncalves-Netto D, Mawatari K and Plehn T 2013 *JHEP* **1301** 148
- [12] Djouadi A, Godbole R , Mellado B and Mohan K 2013 *Phys. Lett. B* **723** 307
- [13] The ATLAS collaboration 2013 ATLAS-CONF-2013-072 (<http://cds.cern.ch/record/1562925>)
- [14] Nason P and Oleari C 2010 *JHEP* **1002** 037
- [15] Hamilton K, Nason P and Zanderighi G 2012 *JHEP* **1210** 155
- [16] de Florian D, Ferrera G, Grazzini M and Tommasini D 2012 *JHEP* **1206** 132